



CHALMERS
UNIVERSITY OF TECHNOLOGY

Hydrometallurgical recycling of steel grinding swarf via hydrochloric acid leaching and precipitation for production of high purity iron chloride

Downloaded from: <https://research.chalmers.se>, 2026-06-18 14:44 UTC

Citation for the original published paper (version of record):

Ottink, T., Petranikova, M. (2026). Hydrometallurgical recycling of steel grinding swarf via hydrochloric acid leaching and precipitation for production of high purity iron chloride coagulants and hydrogen gas. *Resources, Conservation and Recycling Advances*, 29. <http://dx.doi.org/10.1016/j.rcradv.2026.200320>

N.B. When citing this work, cite the original published paper.



Hydrometallurgical recycling of steel grinding swarf via hydrochloric acid leaching and precipitation for production of high purity iron chloride coagulants and hydrogen gas

Thomas Ottink^{*} , Martina Petranikova

Chalmers University of Technology, Department of Chemistry and Chemical Engineering, Kemivägen 4, 41296 Gothenburg, Sweden

ARTICLE INFO

Keywords:

Steel grinding swarf
Recycling
Hydrometallurgy
Iron chloride
Water treatment
Hydrogen gas

ABSTRACT

Grinding swarf is a hazardous waste from the steel and manufacturing industry which is difficult to recycle due to its low value, heterogeneity, and distributed production across numerous workshops. Thousands of tons of grinding swarf are today landfilled, and the aim of this work was to propose an alternative recycling strategy and process for producing iron chloride water treatment coagulants from this waste. Two samples were leached with hydrochloric acid at pH 2 and 60°C for 3 h to extract up to 95% iron from the swarf by forming soluble ferrous chloride (FeCl₂). The slurry pH was thereafter increased to 4 by adding more swarf, at which point chromium, aluminium and molybdenum were precipitated via hydrolysis. Nickel, cobalt, and copper could also be separated from FeCl₂ by precipitation but were instead found to be cemented onto the swarf's metallic iron surface. Nickel and cobalt cementation was facilitated by high chloride concentrations in the slurry. The investigated leaching and precipitation techniques were combined to propose a simple yet flexible process for producing water purification grade iron chloride from grinding swarf. Around 4.2 tons of 34% FeCl₂ solution and 24 kg of hydrogen gas can be produced per ton of swarf as valuable products, promoting recycling and contributing towards zero-waste in the steel value chain.

1. Introduction

Machining processes are essential in the steel and manufacturing industries for shaping, removing defects and finishing surfaces to turn metals into marketable goods. These methods are based on removing excess metal from a workpiece using machining tools and cutting fluids and as such, they generate waste metal chips (swarf) and spent lubricants. Coarse shaping processes, such as turning and milling, produce large metal shavings which are easily recyclable as scrap. Grinding and polishing, on the other hand, generate finer dusts that retain fluids more easily due to their large surface area and form sludges together with the lubricant. This is problematic since high fluid contents generally classify swarf as hazardous waste when common oil-based lubricants are used (EU list of waste, 12 01 18). Moreover, few recycling options are currently available for oil-contaminated swarf and landfilling is today a widespread practice (Großwendt et al., 2023). This poses an environmental threat since leaching of machining fluids and metals from the swarf may contaminate soil and groundwater.

Quantifying grinding waste is challenging due to the widespread use

of grinding in large manufacturing sites and smaller workshops. Chang et al. made a global estimate of an annual 2.3–5.8 million tons of swarf based on cutting fluid consumption in 2006, while Großwendt et al. reported 250 000 tons generated by German industry in 2000 (Chang et al., 2006; Großwendt et al., 2023). These numbers suggest that around 5–6 kg of grinding swarf are generated per ton of crude steel produced based on yearly statistics from the World Steel Association. Assuming that swarf volumes scale with steel production and extrapolating to the current global crude steel market of almost 2 billion tons, puts the total grinding swarf generated at 10–12 million tons per year (World Steel Association, 2022).

Grinding sludges are normally filtered and often also centrifuged or briquetted to remove grinding swarf and recover cutting fluids for reconditioning and reuse (Lee et al., 2017). Dry swarf primarily consists of steel and abrasives and binders from the grinding wheel but can still contain a substantial amount of machining fluids which are difficult to remove mechanically (Hankel et al., 2020). Hydraulic oils from leaking machinery (tramp oils) can often also be found in swarf and are significantly more difficult to remove by briquetting, thereby reinforcing the classification of the material as hazardous waste (Nayström, 1998).

^{*} Corresponding author.

E-mail address: ottink@chalmers.se (T. Ottink).

Glossary

%E	Percentage extracted
E°	Standard potential
EU	European Union
ICP-OES	Inductively coupled plasma optical emission spectroscopy
ISO	International Organization for Standardization
L/S	Initial liquid to solid ratio
SDS	Safety data sheet
T	Temperature
TC	Total carbon
wt-%	Weight percentage
XRD	X-ray diffraction
XRF	X-ray fluorescence

Mineral oils and many additives which form the base of many lubricants have poor biodegradability and are toxic to aquatic life (Wu et al., 2021a). Certain additives and bacteria in cutting fluids are also known to cause detrimental health effects such as dermatitis and respiratory disease. Furthermore, any flammable compounds in the lubricants also make the swarf susceptible to autoignition and swarf has been known to catch fire spontaneously in storage when heat is developed by oxidizing metals (Hess and Kawatra, 1999).

Management of grinding swarf requires sophisticated logistical networks and reliable third-party collection and recycling services. Whilst internal recirculation of swarf is often possible in foundries and steel mills, these conditions are seldom met for manufacturers, leaving landfilling with or without incineration as the sole waste management alternatives. Two main options for recycling are currently available and include remelting swarf briquettes as scrap or the use of swarf as filler in cement (Hankel et al., 2020). Recycling as scrap is preferable to make use of the valuable metallic fraction but requires good briquetting to prevent loose swarf from oxidizing and ending up in slag or furnace dust. This can be difficult to achieve due to moisture, hydraulic oils and oxidation of the metal surfaces which prevents good particle bonding (Nakamura and Hayashi, 2006; Nayström, 1998). Previous and current research is therefore mainly focused on lubricant removal by aqueous washing or supercritical CO₂ extraction with magnetic separation from abrasives and sintering of the metal fraction (Chang et al., 2006; Fu et al., 1998; Großwendt et al., 2023; Lee et al., 2020). While the treatment steps involved are justified for high alloy swarf, most grinding swarf generated industrially contains few valuable alloying elements and limited value is created by simply separating metals, lubricants and abrasives.

The iron and steel industry has historically been based on pyrometallurgy and relies on processing large volumes of material at centralized sites. This makes them less suitable for the recycling of smaller waste streams and materials like grinding swarf are regarded as causing more trouble than they are worth logistically, with risks of contaminating the steel product. Hydrometallurgy has been proposed as an emerging alternative for decontaminating and recovering metals from other steel industry waste streams like furnace dusts and sludges (Binnemans et al., 2020). This method offers an energy-efficient and less capital-intensive solution for processing metals on a small and local scale and is ideal for valorizing metal-containing waste. As far as the authors are aware, no previous attempts to recycle grinding swarf and sludges using hydrometallurgy have been made. An earlier study on the extraction of metals from grinding swarf by hydrochloric acid leaching was published in 2022 by the authors (Ottink et al., 2022). In this work, dissolution of metals and production of iron chloride solutions were investigated at different temperatures, pH levels, and liquid to solid ratios (L/S) using an experimental design. The present research builds upon these ideas

but aims to propose a complete recycling process that was not developed previously.

As steel grinding swarf predominantly consists of iron, it can potentially be used as raw material for iron-based coagulants. Ferric chloride (FeCl₃) and ferric sulfate are used extensively in water treatment with an annual consumption of two million tons in the EU (Incopa, n.d.). This number is expected to increase significantly with new wastewater directives (Directive (EU) 2024/3019) setting stricter limits on emissions of phosphorus, nitrogen, microplastics, and other pollutants from urban environments. Iron chloride can be expected to play a crucial role in this context due to its accessibility, low price, and efficiency as a coagulant (Ramasahayam et al., 2014). Due to the purity requirements in water treatment, these coagulants are today still largely produced from high-grade iron ore. By replacing this natural raw resource with grinding swarf, increased circularity could be achieved in water treatment while promoting swarf recycling via the creation of a valuable product. Considering this, the aim of this work was to investigate whether and how a high-purity iron chloride solution conforming to ISO standards (EN 888:2023) could be produced from grinding swarf. Due to the low value and heterogeneity of the waste, process development was focused primarily on flexibility and simple design.

2. Materials and methods

2.1. Grinding swarf samples

Grinding swarf from the manufacturing of rolling bearings (A) and chainsaw blades (B) were subjects of the study and were provided by SKF AB (Sweden) and Husqvarna AB (Sweden) respectively. The samples were generated in grinding of bearing and low-alloy tool steels with aluminium oxide grinding wheels and semi-synthetic mineral oil-based cutting fluids diluted to 5–6% in water (Castrol, A: Hysol SL 35 XBB and B: Hysol SL 36 XBB). Swarf A was received as filtered and briquetted and was crushed using a mortar and pestle, while B was received as filtered. Air-tight polypropylene containers were used for storage to prevent oxidation.

2.2. Leaching setup and experimental procedure

A jacketed, round-bottom glass reactor vessel (1 L, 10 cm diameter, 20 cm height) was used in all experiments. The reactor was connected to a water bath for heating and was equipped with a polypropylene axial-flow impeller (diameter 7 cm) for stirring at 300–400 rpm with an electric motor. The acidity of the leaching slurry was controlled by measuring pH with a combined glass electrode and by dosing 37% HCl (ACS reagent) with an automatic titrator (Metrohm, Titrando 905) whenever the pH exceeded the desired level. The electrode was calibrated using buffer solutions at the desired experimental temperature before each use, but any effect of the iron chloride electrolyte concentration on H⁺ activity was not accounted for. The REDOX potential was not monitored actively during experiments but was measured using a Pt electrode and found to be -472 ± 10 mV in solutions containing a mixture of >200 g/L FeCl₂ in the presence of grinding swarf at 20°C.

Based on results from previous studies (Ottink et al., 2022), all experiments were conducted at a fixed temperature of 60°C since elevated temperatures had positive effects on metal leaching and separation (Ottink et al., 2022). Higher temperatures may favor dissolution kinetics but were avoided to protect the electrode from thermal damage. Thermodynamic data for chemical reactions such as Gibbs free energies were calculated with HSC Chemistry 10.

Unless mentioned otherwise, the reactor was initially charged with 300 mL of water which was preheated to 60°C. Varying amounts of swarf were then added to the solution to give a predetermined liquid-solid ratio (L/S), and experiments were started by commencing acid dosing. Aliquots of the aqueous phase were taken during and after leaching and prepared for Inductively Coupled Plasma Optical Emission

Spectroscopy (ICP-OES, ThermoScientific iCAP PRO) analysis by filtration with $a < 45 \mu\text{m}$ PES syringe filter and dilution in 0.1 M HNO_3 (Puriss, 65%). To determine the extractability of different metals, leaching efficiencies were calculated using Eq. (1).

$$\%E = 100 \cdot \frac{C_M V_l}{m_s x_M} \quad (1)$$

where C_M is the concentration of metal M in the leachate with volume V_l , and x_M is the mass fraction of M in the swarf of mass m_s , originally added to the reactor. Volume losses due to sampling and evaporation were accounted for with an evaporation rate of 12.5 mL/hour at 60°C based on heating and stirring water in the reactor over 4 h. Residual solids after leaching were separated with vacuum filtration using glass fiber filters (Whatman) and washed with 100 mL water before drying in a fume hood for 24 h.

2.3. ICP-OES calibration and analysis

Due to large differences in Fe and impurity concentrations, two separate calibration standards were prepared for ICP-OES analysis. Iron solutions of 0.625–20 ppm were prepared by diluting 1000 ppm Fe (Teknolab Sorbent AB) in 0.1 M HNO_3 . Standards of the same concentrations were prepared for impurities; however, these and a blank were dosed with 5000 ppm Fe (FeCl_2 from leaching tests) to account for matrix effects from high iron chloride concentrations. By ensuring that standard and sample matrices were comparable, any matrix effects should be the same in each set. This enabled the use of calibration curves for determining sample concentrations. Any impurities (Mn, Ni, etc.) in the added FeCl_2 in standards were accounted for in evaluations of each standard's measured intensities by subtracting the measured blank values. Samples from leaching were diluted to ensure that metal concentrations were within range of the respective calibration standards.

2.4. Characterization of solids

Swarf and solid residues were quantitatively analyzed with wavelength dispersive X-ray fluorescence (XRF, Panalytical Axios) with a Rh anode, where solids (2–4 g) were loaded in polypropylene containers and exposed through a 6 μm film in a He atmosphere. Qualitative analysis was performed by X-ray diffraction (XRD, Bruker D8 Discover) using a Cu source with wavelength 1.5406° and 2θ between 10–80° with 0.04° increments at 0.04°/s. Optical microscopy and SEM (Phenom ProX™) were also utilized to study the swarf shaving's physical structures and particle sizes.

The steel fractions in the swarf were further analyzed by dissolving triplicates of 0.5 g swarf in 30 mL in aqua regia (3:1 HCl (ACS reagent, 37%): HNO_3 (Suprapur, 69%)) for 2 h at 80°C. Each solution was thereafter made up to 50 mL with Milli-Q water, and aliquots were filtered through a 0.45 μm polypropylene syringe filter, further diluted in 0.1 M HNO_3 , and analyzed by ICP-OES.

Cutting fluid contents in swarf were estimated by gravimetric analysis after at least 5 cycles of Soxhlet extraction with ethanol (Solvenco analytical grade, 95%) in cellulose thimbles. To distinguish water content from organic lubricants, Dean-Stark moisture determination was performed by boiling swarf with toluene (anhydrous, 99.8%) and weighing the extracted water. Further carbon combustion analysis (LECO CS744) of swarf was also performed to estimate total carbon (TC) contents.

3. Results and discussion

3.1. Swarf characteristics and chemical compositions

Despite appearing macroscopically like a powder material, the swarf was made of microscopic, intertwined shavings, giving it a characteristic

fluffy texture. Optical microscopy images of the two grinding swarf samples and a typical SEM image of swarf A can be seen in supplementary Figure S5. No significant differences in particle size were observed, although as can be expected, briquetted swarf A was denser than the non-briquetted swarf B. A closer look with SEM revealed the sickle-shaped structure of the shavings with approximate length $< 100 \mu\text{m}$, width $< 20 \mu\text{m}$, and thickness of $< 1 \mu\text{m}$. The metallic gleam of the shavings suggested that the steel was mostly unoxidized, which was confirmed with XRD (see Fig. 3). Slight differences in steel compositions were observed where sample A was a blend of ferritic and austenitic crystalline phases whereas B was mainly ferritic. Alumina abrasives were present in both samples and these particles were not metallurgically bonded but can be trapped within the sickle-shaped steel and are difficult to separate completely (Großwendt et al., 2023).

Chemical compositions of swarf A and B are given in Table 1. Elemental contents of the steels were determined by aqua regia digestion and ICP-OES, and validated with XRF, while abrasives (Al_2O_3) and other metals were quantified solely using XRF. The total cutting fluid and water contents are based on single Soxhlet washing and Dean-Stark extraction procedures. Total carbon (TC) was determined with combustion analysis and is the total of inorganic carbon from steel and organic carbon from cutting fluids, tramp oils, and abrasive binders. Although reported standard deviations in Table 1 are small, grinding swarf is generally inhomogeneous and relative quantities of steel, abrasives, cutting fluids, and tramp oils may vary between batches. This is due to hydraulic oil leaks, periodic dressing of the grinding wheel, mixing of swarf from different production lines, etc. Sampling over a longer period is required to reflect average compositions (Azarhoushang, 2022).

Similar steel alloying elements were found in low quantities in each swarf, with slightly more Cr and Mn in A and more Ni and Al in B. Swarf A also contained 0.09% Mo, which was not found in swarf B. The high Fe content in sample A is explained by residual cutting fluid contents where filtered sample B contained 25.2% fluids, of which 19.5% water, whereas briquetted swarf A only contained 6.2% of which 3.7% water.

A summary of the organic lubricant components based on safety data sheets (SDS) is given in supplementary materials Table S2. Both lubricants had a base of 25–50% mineral oil with various amines, carboxylic acids, and long-chain alcohol additives for corrosion inhibition, pH regulation, emulsification, defoaming, etc. Besides these original components, tramp oils and various decomposition products may also be present.

Table 1

Chemical compositions of grinding swarf A and B with elemental compositions of the steel on the left hand, and abrasive and cutting fluid contents on the right hand. Other components may include alkali and alkaline earth metals (Na, K, Ca, Mg), C, S, P and O.

Steel	Abrasives, cutting fluids & other				
	Element	Component	A (wt-%)	B (wt-%)	
Fe	78.4 ± 0.8	68.4 ± 1.9	Al_2O_3	7.75 ± 0.08	3.1 ± 0.05
Cr	1.13 ± 0.01	0.41 ± <0.01	SiO_2	0.72 ± 0.03	0.61 ± <0.01
Mn	0.37 ± <0.01	0.23 ± <0.01	Cutting fluid	~6.2	~25.2
Ni	0.10 ± <0.01	0.64 ± <0.01	Water*	~3.7	~19.5
Cu	0.10 ± <0.01	0.04 ± <0.01	Lubricant*	~2.5	~5.7
Mo	0.09 ± <0.01	<LOD	TC	6.11 ± 0.17	2.45 ± 0.15
Al	0.04 ± <0.01	0.19 ± <0.01	Other	4.9	1.1
Co	0.01 ± <0.01	0.01 ± <0.01			

* Subcomponents of Cutting fluid.

A notable difference in Table 1 are the TC contents, which do not match the estimated amount of lubricant in each sample. Assuming carbon contents in the steels are similar, less TC was expected in swarf, and this sample may have contained organic binders from the grinding wheel or tramp oils. Bakelite and polymeric resins are common binders in abrasive wheels and are released into the sludge when grinding, contributing to the carbon content of the swarf (Webster and Tricard, 2004). Tramp oils are another carbon source that is difficult to remove from the swarf mechanically, even with briquetting (Nayström, 1998). The latter were likely to be present in sample A, judging from a faint oily smell on this swarf after Soxhlet extraction. The Hysol SL 35 XBB lubricant was found to be readily soluble in ethanol, whereas less polar hydraulic oils may not have been. Both heavy oils and polymers can also account for the high concentration of other unidentified substances in sample A.

To summarize, steel fractions were comparable both physically and chemically between samples. Swarf A had a denser structure and lower cutting fluid content due to briquetting, but contained more grinding wheel binders and abrasives, and tramp oils, whereas B was fluffier with a high cutting fluid content. Due to similarities between steels, similar leaching behaviors were expected, and any effects of cutting fluids on the dissolution process should be distinguishable.

3.2. Recycling process development

Developing a recycling process for iron chloride production from grinding swarf was centered around metal separation with economically and technically feasible solutions to minimize the overall costs of the technology. To achieve a commercially viable product, the research was divided into two steps. The first step was to establish an efficient technique for dissolving and separating Fe from Cr and other metals based on previous leaching studies (Ottink et al., 2022), aiming at commercial FeCl₃ metal impurity limits (EN 888:2023). Secondly, a method for producing concentrated iron chloride solutions conforming to industrial standards of 40 wt-% FeCl₃ was investigated.

3.2.1. Leaching principles and hydrolysis precipitation

The main mechanism behind leaching of Fe from grinding swarf with HCl and producing ferrous chloride (FeCl₂) and hydrogen gas (H₂) is given in Eq. (2), which is spontaneous at standard conditions with $\Delta G^\circ = -44.8$ kJ/mol.



This reaction leads to significant H₂ bubbling in the solution. In the presence of air, Fe(II) may further oxidize spontaneously to Fe(III) by reacting with dissolved oxygen via Eq. (3) with $\Delta G^\circ = -330.8$ kJ/mol.



This process is slow in acidic solutions due to the limited solubility of O₂ and the dominance of uncomplexed Fe²⁺, but at intermediate pH levels, formation of the more easily oxidized hydrolysis products FeOH⁺ and Fe(OH)₂ speeds up the reaction (Morgan and Lahav, 2007). Though FeCl₃ is the desired final product, its formation is unwanted from a hydrometallurgical perspective since Fe(III) is more easily precipitated as FeO(OH) with oxygen or Fe(OH)₃ without oxygen at pH >3.5 (Niu et al., 2021). Fortunately, metallic Fe in the grinding swarf stabilizes Fe(II) by spontaneous reduction of Fe(III) via Eq. (4) with $\Delta G^\circ = -124.7$ kJ/mol, which minimizes or eliminates the risk of Fe loss even at intermediate pH levels of 4–5 (Ottink et al., 2022).



This previous work also showed that near-complete dissolution of Fe was possible for grinding swarf A at pH 2–3 and 60°C within 3 h. Under these conditions, significant co-dissolution of unwanted Cr and Ni can however also be expected. At pH 4, selective leaching of Fe over Cr is

possible, but the dissolution becomes slow and inefficient. The mechanisms behind this selectivity were not fully investigated and are either explained by difficulties with dissolving metallic Cr in dilute HCl or, more plausibly, that Cr is continuously dissolved as Cr(III) and precipitated as Cr(OH)₃ by hydrolysis via Eq. (5) (Rai et al., 1987; Shen et al., 2008).



Though this reaction is non-spontaneous at standard conditions with $\Delta G^\circ = +62.8$ kJ/mol, Pourbaix diagrams show that Cr(OH)₃ is predominant at pH 4.3–5.5 and could be precipitated (see supplementary material Figure S6). To test the latter theory, triplicate precipitation tests were performed where swarf A was leached at pH 2 and L/S = 10 mL/g for 3 h, after which the slurry pH was incrementally increased by consuming excess HCl with 1 g grinding swarf additions via Eq. (2). Metal concentrations at increasing pH values are shown in Fig. 1 where each level was maintained for 30 min before sampling. Adjustment of pH with NaOH was ineffective and resulted in Fe(II) precipitation.

Many alloying elements dissolved with Fe and were stable until pH 3.5. At pH 4–4.5, a decrease in Cr, Al and Mo concentrations can be observed which confirms that Cr is dissolved and likely precipitated via Eq. (5). Similar precipitation mechanisms are probably for Al and Mo, which have been shown to hydrolyze and precipitate between pH 4–5 in chloride media although a coprecipitation mechanism with Cr cannot be ruled out (Huang et al., 2004; XIAO et al., 2008). Regardless, Al and Mo are of little concern in coagulant production, and their precipitation mechanisms were not explored further.

Fig. 1 also shows no reduction of Fe, Mn, Ni, or Co concentrations throughout the experiment. This is in line with Hard and Soft Acid and Base (HSAB) theory, where Cr³⁺ and Al³⁺ are hard acids with higher affinity for OH⁻, while the borderline acids Fe²⁺, Mn²⁺, Ni²⁺, and Co²⁺ should be more difficult to hydrolyze (Pearson, 1963).

3.2.2. Consecutive leaching and precipitation

Based on these results, it should be possible to achieve high Fe leaching efficiencies without compromising Cr separation by splitting the dissolution process into a leaching and precipitation step. This was tested on both samples A and B to determine whether the method can be applied more generally for grinding swarf originating from different sources.

Each swarf was first leached for 3 h at pH 2 with L/S = 10 mL/g, followed directly by precipitation for 1 h at pH 4, and the extraction

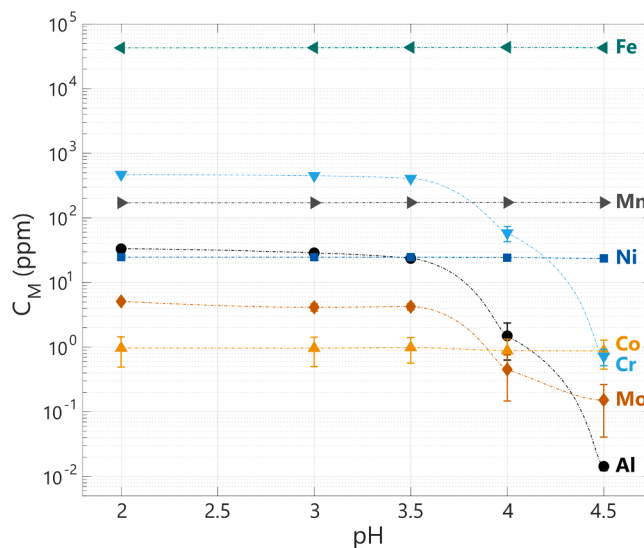


Fig. 1. Metal concentrations in a leaching slurry based on swarf A when incrementally increasing pH from 2 to 4.5 at 60°C.

efficiencies over time are shown in Fig. 2a and b. Despite similarities between steel shavings, large differences in leaching behaviors were noted, namely only 45% of Fe in sample B was dissolved while >90% was dissolved for A. Two other key observations for B were that no Cr was dissolved, and Al efficiencies started at 100%, decreased to 80% during leaching, and were further reduced to 0% after precipitation.

Efficiencies for Cr are explained by examining the respective steel workpieces. Swarf B was generated in the sharpening of chainsaw chain links, which had been electroplated with Cr for corrosion protection prior to grinding. Since Cr is easily oxidized to corrosion-resistant Cr₂O₃ in air, most Cr in sample B can be assumed to be insoluble in dilute HCl. In swarf A from bearing steel, Cr was present as an alloying element and was thus left mostly unoxidized and more readily soluble via Eq. (6) with ΔG° = -222.9. kJ/mol.



Analogously to Cr, Al existed both as an alloying element in the steel and as insoluble Al₂O₃ in the form of abrasives. Based on the dissolution trends for Fe and alloying elements in Fig. 2a, any Al measured by ICP-OES likely came from the steel. For swarf B, it was probable that microscopic (<45 μm) suspended abrasive particles capable of passing syringe filters caused high readings in ICP-OES analysis. This apparent Al concentration decreased slightly due to a volume increase during leaching, whilst during the following precipitation, any Al₂O₃ particles were coagulated by precipitating metals and became non-filterable (Atkins and de Paula, 2002).

Further considering efficiencies for Fe, Co, Mn, and Ni in Fig. 2b, it is clear that swarf B was only partially dissolved compared to swarf A. This was also observed experimentally, where metal shavings were largely intact when filtering the leachate from swarf B, whereas residues from A were a dark sludge. After drying, both residues had turned brown, a color indicative of iron hydroxide and oxide formation. Washed and dried filter cakes were analyzed with XRD to study leaching residues

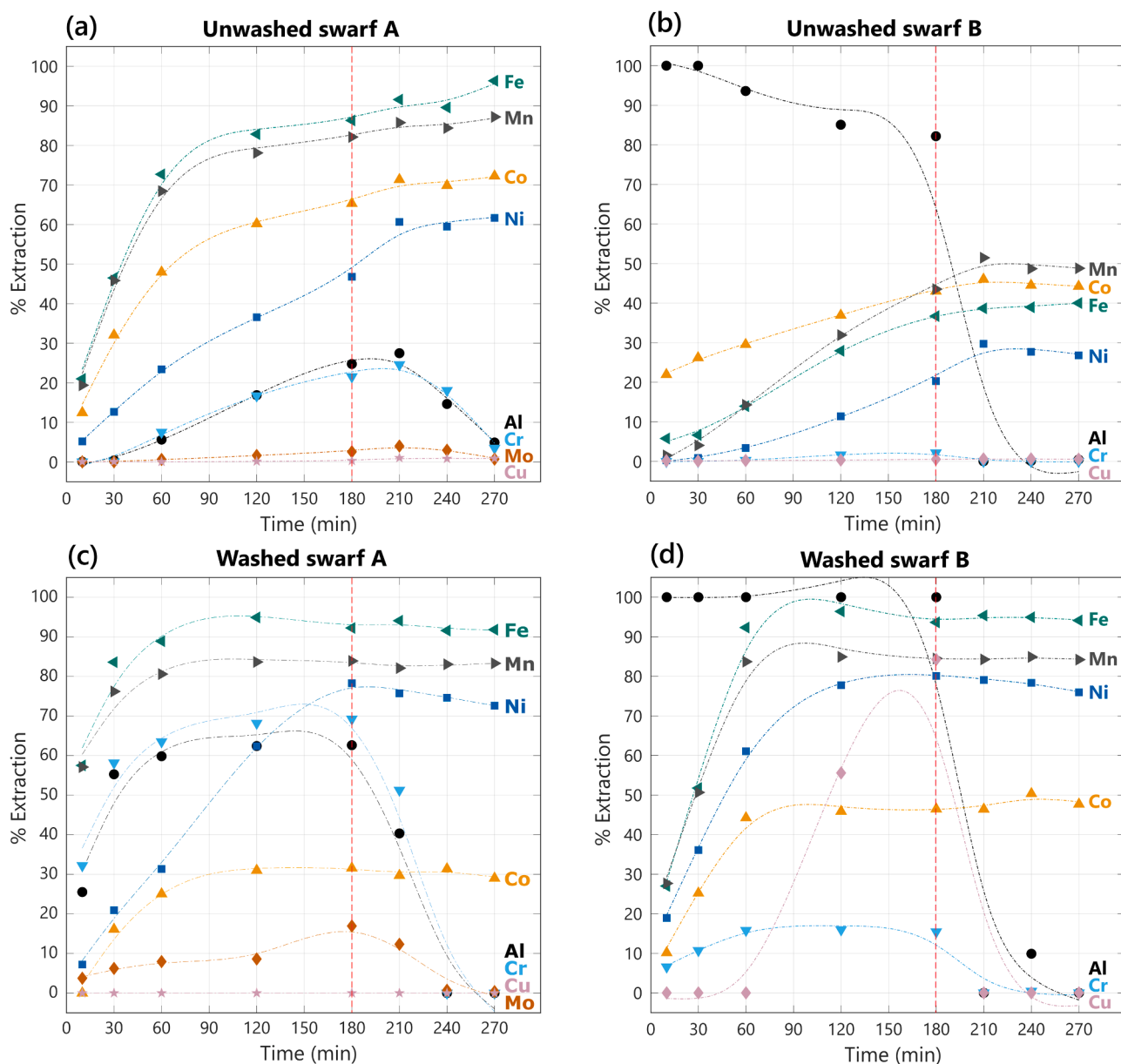
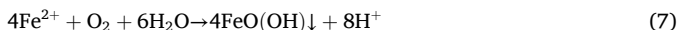


Fig. 2. Consecutive leaching of grinding swarf A (a) and B (b) for 3 h at pH 2 and 60°C follow by precipitation at pH 4. Identical experiments were also performed with ethanol washed swarf A (c) and B (d) for which reference metal contents in solids are found in Table S3. Vertical red lines mark the addition of swarf for precipitation.

with patterns for untreated swarf as a comparison in Fig. 3.

Residues from swarf A in Fig. 3a show that ferrite and austenite were almost completely dissolved and revealed cementite, which was evidently present in low quantities in the steel. Cementite has a relatively high carbon content, which presumably protected the remaining Fe and made it inaccessible to HCl. Some lepidocrocite was also observed and was likely formed by oxidation and hydrolysis of FeCl_2 in the filter cake during air drying via Eq. (7).



Which is spontaneous with $\Delta G^\circ = -267.7 \text{ kJ/mol}$. No Cr compounds were observed in Fig. 3a, which confirms that Cr was indeed precipitated as amorphous $\text{Cr}(\text{OH})_3$ (Rai et al., 1987).

Swarf B was less affected by leaching and the ferritic structure was largely intact. According to Fig. 3a ferrite should have been dissolved easily by HCl, which suggests that the steel surfaces were likely passivated and protected in some way. The contents of alloying elements such as Cr and Ni were too low to provide any significant corrosion protection (Einar Mattsson, 1996), suggesting that the cutting fluids may have interfered with the leaching process. Swarf A contained significantly less lubricant compared to B as a consequence of briquetting. This can be of importance since water-based cutting fluids normally contain corrosion inhibitors, which serve to protect the workpiece during machining but incidentally also prevent corrosion of the grinding swarf (Einar Mattsson, 1996). The corrosion-inhibiting effects of cutting fluids were validated by washing grinding swarf with ethanol before leaching, which resulted in near-complete dissolution of the steel fractions, according to Fig. 2c and d.

It has now been shown that simply filtering grinding sludges may not remove sufficient cutting fluid to allow efficient iron dissolution. Thus, additional pretreatment by briquetting or centrifugation is necessary. Some more attention will now be given to the lubricant oils to give a better understanding of their behavior and fate in the leaching, precipitation, and filtration steps.

3.2.3. Oil demulsification and coagulation

Grinding swarf initially released cutting fluids when mixed with water solutions, giving a milky color from emulsified oils. This was especially true for swarf B, which produced highly turbid solutions. After approximately one hour of leaching, the aqueous phase cleared, and the filtered leachate was completely transparent and without an oil film (see supplementary Figure S7). This suggests that the oils were demulsified by coagulation or flocculation (Atkins and de Paula, 2002).

Hydrophobic oils and emulsifiers from cutting fluids form colloidal droplets in water, which are stabilized in the solution by an electrical double layer with potential ζ , causing them to repel similarly charged particles (Atkins and de Paula, 2002). When the ionic strength is increased by the introduction of an electrolyte such as FeCl_2 , ζ is minimized, allowing colloids to aggregate by coagulation or flocculation. Aggregation is facilitated by several factors, including ionic strength, elevated temperatures, agitation, and metal hydrolysis (Guimarães

et al., 2010; Ríos et al., 1998). These prerequisites are fulfilled in the leaching and precipitation system, demulsification of oils should be highly effective.

During leaching, precipitation, and filtration, a thin oil film was barely visible on the slurry surface, indicating that some secondary phase formation indeed took place. However, no such layer was visible on filtered FeCl_2 solutions. This suggests that any aggregated oil was consecutively adsorbed by the filter cake. Despite the fact that most hydrophobic substances tended to stay in the filter cake, water-soluble components of the semi-synthetic fluids may still have ended up in the FeCl_2 solution, as indicated by a fishy odor stemming from the solution.

To conclude this section, splitting the leaching process into two steps made efficient extraction of Fe with separation from Cr, Al, and Mo possible. The resulting process was also capable of removing any hydrophobic substances from the formed FeCl_2 solution but corrosion inhibitors and oils in the lubricants can contribute to decreasing metal leaching efficiencies. Thus far, a solution containing 50 g/L Fe (10 wt-% FeCl_2), with Ni concentrations exceeding allowable trace metal limits had been produced. Concentration of the FeCl_2 solution from swarf A was investigated next in an attempt to get closer to the commercial standard of 40 wt-% FeCl_3 .

3.3. Concentration of the iron chloride solution

There are many ways to concentrate a leachate, including water evaporation, lowering L/S ratios, and leaching at higher acid concentrations to avoid dilution. To keep processing costs and energy consumption low, two simple methods were primarily tested: minimizing L/S ratios and leachate recirculation. The concentration of dosed HCl was already at the highest commercially available level and could not be increased further.

Several L/S ratios of 1, 2, 3, 5, and 10 mL/g were tested in this study. The main issue with lowering L/S is that grinding swarf has a high capacity to retain fluids and acts like a sponge when wetted. This makes mixing more difficult and creates an expanding foam that is lifted when H_2 is formed. The foam generally remained for about an hour before disintegrating, allowing the remaining swarf to be mixed into the slurry. At L/S = 1–2 mL/g, swarf A absorbed the entire initial liquid volume and became an unmixable sludge which overflowed upon HCl addition due to gas formation. A good compromise was found at L/S = 3 mL/g, resulting in manageable frothing and final Fe concentrations around 150 g/L (27 wt-% FeCl_2).

3.3.1. Recirculation of leachate

Recirculation was tested by reintroducing filtrate from previous tests as a starting aqueous phase in new leaching experiments. A more descriptive representation of this recirculating flow is shown in Fig. 5. To study how leaching and precipitation were affected by stepwise increases in FeCl_2 concentration, L/S = 5 mL/g rather than the optimal 3 mL/g was used in these tests. Graphs showing metal concentrations, pH, and total HCl volumes added over time for three recirculations (R0, R1,

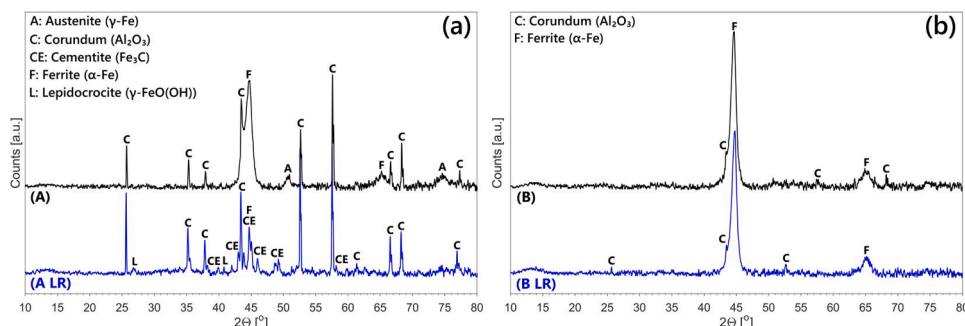


Fig. 3. XRD analysis of untreated swarf A (a) and B (b) and their respective leaching residues (LR) with patterns of swarf at the top and leaching residues below.

and R2) are given in supplementary Figure S8. The first leaching test, i. e., R0, was started with 300 mL of water.

In general, the leaching and precipitation performed as expected with final Fe concentrations of 110 g/L (21 wt-% FeCl₂) in R0, and 185 g/L (31 wt-% FeCl₂) in R1, respectively. Concentrations of Cr, Al, and Mo dropped to near-undetectable levels at pH 4 in each case. The pH at which hydrolysis of these metals occurred therefore seemed to be independent of FeCl₂ concentration. In R2, the Fe concentration reached 249 g/L (39 wt-% FeCl₂) after leaching but in this case, pH was more difficult to adjust by simply adding swarf and leveled out at pH 3.8. A possible reason for this was that the reaction between Fe and HCl in Eq. (2) was close to equilibrium and hence less efficient. Another theory was that Fe²⁺ and its chloro-complexes were hydrolyzed more easily at high FeCl₂ concentrations, releasing H⁺ into the solution and thereby preventing neutralization of the acid. The latter also occurs in concentrated FeCl₃, making these salt solutions relatively acidic (Jamett et al., 2018). Regardless of the underlying mechanism, a high FeCl₂ content interfered with impurity precipitation, and since the goal was to reach pH 4 without additional chemicals, water was added to dilute the FeCl₂, giving a final Fe concentration of 210 g/L and pH 4. This may set an upper limit on the FeCl₂ concentration for precipitation of Cr via pH control.

The theoretical amount of 37% HCl required for swarf containing 78% Fe (disregarding alloying elements) was 2.33 mL/g. For experiments with 60 g swarf, this meant a consumption of 140 mL HCl was expected. In reality, 131 mL was added in R0, 125 mL in R1, and 113 mL in R2. This decrease could not be explained by variations in the swarf composition. To stabilize the FeCl₂ product, additional HCl was added between recirculations, and a week passed between experiments, during which FeCl₃ may have been formed. Both HCl and FeCl₃ may have reduced the acid demand to a minor extent.

More likely, the acid consumption was affected by higher FeCl₂ concentrations, either through reduced dissolution or hydrolysis of Fe. Elevated Fe concentrations could for instance have created more favorable conditions for the hydrolysis of Fe²⁺. This can contribute to leaching by partial hydrolysis of the aqueous Fe via Eqs. (2) and (8).

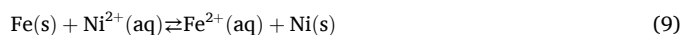


Acid released by hydrolyzing species thus aids the extraction of Fe, which ties in well with the observed difficulty to adjust pH in R2. Recirculation of FeCl₂ can also lead to the accumulation of corrosion inhibitors. These then protect the steel more effectively when FeCl₂ is concentrated. To test this, leaching efficiencies for Fe were calculated from ICP-OES data for R0, R1, and R2, which indicated that nearly all Fe

was extracted during leaching in each case. The latter theory was thus unlikely, and the reduced acid consumption was mainly caused by hydrolysis of the Fe product.

3.3.2. Cementation of Ni and Co with increasing FeCl₂ concentrations

Another trend that was more difficult to discern in recirculation experiments was a relative decrease in Ni and Co concentrations. This is revealed in Fig. 4, where a decrease in Ni at high FeCl₂ concentrations is seen. The trend for Co is similar but less dramatic, with Co/Fe ratios of 136 mg/kg in R0, 125 mg/kg in R1, and 106 mg/kg in R2. This is due to cementation via Eq. (9) and is driven by differences in reduction potential between Fe²⁺ and Ni²⁺ and Co²⁺.



A similar deposition of Cu on the steel surface also occurs, but is more efficient due to a large difference in reduction potential between Fe and Cu (Miller and Beckstead, 1973). Standard reduction potentials for half-cell reactions in Eqs. (11)–(12) in acidic media are E° = -0.44 V, E° = -0.23 V and E° = -0.28 V respectively.



Since cell potentials for Ni (+0.21 V) and Co (+0.16 V) cementation are positive at standard conditions, deposition should occur spontaneously, but it is slow due to rate limitations and redissolution by HCl at moderate FeCl₂ concentrations. Cementation is often described as a mass transport-limited process with diffusion of the depositing metal to the surface as the rate-limiting step. Electrochemical studies however suggest that the rate is governed by mixed control depending on the deposition surface availability, and the types of sacrificial metal and supporting electrolyte (Sareyed-Dim, 1974; Sędzimir, 2002). Elevated temperatures generally promote both kinetics and mass transport and can be expected to have a positive effect on the removal of Ni and Co in the process, despite not being tested in this study to avoid damage to the pH electrode.

Greater access to metallic Fe surface in recirculation experiments due to lowered L/S likely had a positive influence on impurity cementation, but the rate limitations were clearly also less pronounced in highly concentrated chloride media. This phenomenon has also been observed previously in sulfate and nitrate systems, but has proven to be most efficient with chlorides (Addy and Fletcher, 1987; Lienhardt, 1925;

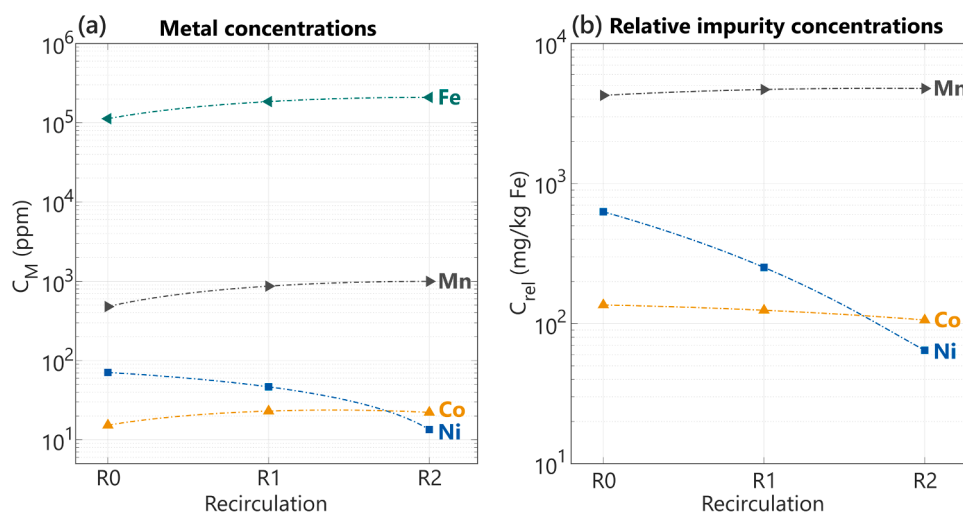
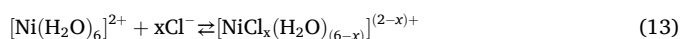


Fig. 4. Metal concentrations in filtrates from recirculations R0, R1 and R2 (a) and impurity concentrations relative to Fe in mg/kg in each solution (b). Experimental data was fitted with a smoothing spline function to show trends.

Sareyed-Dim, 1974; Saylam, 1982). A common explanation is that chlorides remove passivating oxide layers and produce fast-growing, porous dendrite formations at which metals can be adsorbed (Winand, 1991). This creates larger surface areas for deposition, which in turn reduces mass transport limitations, leading to mixed or kinetic control.

On a molecular level, two additional positive indirect effects from chloride ions are generally proposed in surface reduction of Ni: adsorption of Cl⁻ ions on the cathode surface (Jinxing, 1982), and formation of more easily adsorbed Ni chloride complexes (Winand, 1991). With increasing Cl concentrations, coordinated water around the Ni²⁺ ion can be replaced to form NiCl⁺, NiCl₂⁰, and NiCl₃⁻ via Eq. (13) (Liu et al., 2012).



Despite having >7 M Cl in the concentrated FeCl₂ solution, chlorination of Ni can be assumed to be limited in this case. The formation constants for higher order complexes are small at <100°C and Fe(II) has a higher affinity for Cl⁻, which lowers its availability (Winand, 1991). Likely Ni species in the system thus include Ni²⁺, NiCl⁺, and possibly uncharged NiCl₂⁰. Adsorption of Cl⁻ at the cathode can reduce transport resistances of the positively charged Ni(II) complexes through the electrical double layer and may therefore increase cementation rates. The NiCl⁺ ion can also be reduced via a different mechanism than Ni²⁺ in two steps described by Eqs. (14) and 15 (Winand, 1991).



The second Ni(I)/Ni step is independent of Cl⁻, whereas the former Ni(II)/Ni(I) reduction involves side reactions with Cl⁻ and has proven to be significantly faster than adsorption of Ni²⁺ (Hurlen, 1975). Another effect of Cl⁻ is a shift in reduction potentials for Ni(II)/Ni at high ionic strength. Winand reported potentials as high as $E = -0.058$ V vs SHE in 4 M NaCl+0.5 M HCl solutions at 30°C with only a slight shift for Fe(II)/Fe to $E = -0.46$ V vs SHE, which makes redissolution by H⁺ or reverse cementation less thermodynamically favored (Winand, 1991). Similar mechanisms can be assumed to hold for Co and, based on standard reduction potentials for other metals, cementation may also represent a solution for removing other nobler contaminants such as Hg, Pb, Sn, and Cd from FeCl₂ solutions (Anacleto and Carvalho, 1996; Makhloufi et al., 2000).

3.4. Final products and proposed recycling process

Final metal concentrations in filtrate from R2 are given in Table 2 and show that relative metal impurity concentrations (mg/kg Fe) were close to the highest EU standards (EN 888:2023) for drinking water

Table 2

Composition of filtrate R2 (FeCl₂) in comparison with allowed impurity concentrations in commercial FeCl₃ for drinking water applications according to standard EN 888:2023. Entries with n/a signify that no upper limits are given in the standard.

Element	Concentration (mg/L)	Purity of R2 (mg/kg Fe)	Type 1* (mg/kg Fe)	Type 2* (mg/kg Fe)	Type 3* (mg/kg Fe)
Fe	210 000	-	-	-	-
Mn	998	4773	5 000	10 000	20 000
Co	22	106	n/a	n/a	n/a
Ni	14	65	60	350	500
Cr	5	26	50	350	500
Cu	4	20	n/a	n/a	n/a
Mo	4	17	n/a	n/a	n/a
Al	<1	<1	n/a	n/a	n/a
TOC	550	2630	n/a	n/a	n/a

* 40 wt-% FeCl₃ solution basis.

purification. Manganese is of lesser concern, but swarf with a high Mn content may be less suitable as, leaching cannot be avoided. The same is true for Ni and Co, but the process is more flexible in this regard when operating at high FeCl₂ concentrations and temperatures due to more efficient cementation under these conditions. For Cr, Mo, and Al, the process has proven highly flexible, with guaranteed low final concentrations when the FeCl₂ concentration is kept within limits where a final pH of 4 can be guaranteed.

In addition to metal impurities, Table 2 shows that the recycled FeCl₂ solution with a TOC of 550 mg/L also contained some water-soluble organics from cutting fluids. A carbon balance for the process based on 6.11% TC in swarf A and a TOC of 550 mg/L in the output indicated that only 3% carbon from the swarf was transferred to the FeCl₂ solution (4.2 kg/kg input swarf). In terms of functionality, these remaining substances don't form a hindrance in water treatment applications. This has been proven by oxidizing FeCl₂ to FeCl₃ and performing flocculation tests with an industrial partner (Kemira Kemi AB). These results are presented as supplementary material and prove that the performance of recycled FeCl₃ was comparable to a magnetite-based product. Since coagulants are generally added in small doses in the first stages of water treatment, it is also reasonable to assume that organics stemming from the coagulant will be taken care of e.g., in the following biological processes. Practically, iron chloride consumers may however be suspicious of unusual smells, and deodorization of the product may be required even though there are no specific limits for organic impurities given by the EN 888:2023 standard.

A few words should be said about the oxidation of the recycling product since FeCl₂ is of lesser industrial importance than its FeCl₃ counterpart even though it has some specialty applications as a coagulant in e.g. chromate precipitation (Wildermuth et al., 2000). Historically, the preferred method for oxidizing FeCl₂ solutions is using chlorine gas (Crabtree and Schaefer, 1966). This method is practical since it doesn't dilute the FeCl₃ product but comes with health and safety concerns. There are several alternatives to Cl₂, which include chloride-based oxidizers such as hypochlorite (ClO⁻) and chlorate (ClO₃⁻), and oxidizers used in combination with HCl as a chloride source, which include hydrogen peroxide (H₂O₂), ozone (O₃), and oxygen. The latter introduces significant amounts of water in the product from aqueous HCl, but oxidation with pressurized oxygen is today the industrially preferred method due to its low cost and environmental footprint (Johansson and Liljenroth, 2023; Swaminathan et al., 1981). For FeCl₂ containing organic contaminants, partial oxidation with H₂O₂ or O₃ could be ideal to simultaneously oxidize Fe(II) and remove TOC and odors via advanced oxidation mechanisms (Wu et al., 2021b). Regardless of the method selected, pure chemicals should be used to avoid contaminating the FeCl₂, and precipitation of Fe should be avoided to prevent the loss of product and an increase in relative metal impurity concentrations.

3.4.1. Solid residue composition and characteristics

Analysis of dried solid residue compositions based on XRF and carbon analysis is presented in supplementary Table S4 along with XRD analysis of residue from R0 and R2 in Figure S9. Contents of FeO(OH) in solid residues increased from 40% in R0 to 47% in R1 and 58% in R2. This was either due to precipitation of Fe during leaching, precipitation or filtration, or more FeCl₂ remaining in the residues after filtration and washing of the filter cake. Despite an observed increase in Fe content, filter cakes generally weighed half of the input amount of swarf. Hydrolyzed precipitates and Cl salts predominantly contribute to the mass, along with grinding wheel abrasives and organic binders, and lubricants.

In terms of waste management, the economic incentive for recycling solid residues may be higher than for swarf, since valuable alloying elements are concentrated during leaching. Several commercial shaft or blast furnace processes (Oxycup, DK-process, Scandust, etc.) that specialize in making steel from dust and sludges are available, where the

high carbon content could provide a reduction and/or energy source, and Cr, Ni, and Mo are desirable for making high alloy steels. Storage of solid residues is also safer than grinding swarf since metals are already oxidized, which eliminates the risk of fires by self-ignition.

3.4.2. Proposed process flowsheet and material balances

Based on the work in this study, a flowsheet for recycling of grinding swarf for production of FeCl_2 solutions as a precursor to FeCl_3 coagulants is proposed in Fig. 5. The process is easily operated in batch in a single vessel, and temperatures $\geq 60^\circ\text{C}$ should be maintained to promote dissolution, hydrolysis, and cementation during dissolution and precipitation. By leaching at $\text{pH} \leq 2$ and precipitating at $\text{pH} \geq 4$, efficient Fe dissolution and complete precipitation of Cr, Al, and Mo is achieved. Operating at the lowest feasible L/S ratios and partially recirculating FeCl_2 filtrate ensures high chloride concentrations with maximum Ni, Co, and Cu cementation and good oil separation. All of these impurities can then be removed by filtration.

A mass balance calculation sheet for the recycling process is shared separately as supplementary material. As a basis for calculations, the grinding swarf was assumed to be leached without any prior washing. Other minor assumptions are presented directly in the calculation sheet. Modelling of material flows based on experimentally observed solid residue mass and iron content revealed that the overall recovery efficiency for Fe was around 85%. A priority for process optimization should thus be to eliminate losses during leaching, precipitation, filtration, and filter cake washing. Good starting points to prevent precipitation of the FeCl_2 product during filtration include minimizing exposure to air to prevent oxidation to unstable Fe(III) and washing the filter cake with slightly acidified water. Other materials, such as lubricants and abrasives, can also be separated out by washing and magnetic separation prior to hydrometallurgical processing to increase leaching efficiencies and reduce secondary waste filter cake.

Under the assumption that the process is started with 1 ton of swarf containing 78% Fe and has an expected iron recovery efficiency of 85%, an input of 2.34 tons of 37% hydrochloric acid and 1.34 tons of makeup water is required. The product output is then 4.21 tons of 34% FeCl_2 solution. An alloy concentrate of around 0.5 tons is also obtained based on empirical data, and a theoretical 24 kg H_2 can be expected, assuming that the dissolution occurs mainly via Eq. (2). These byproducts could, for example, be circulated back to the steel industry. The relatively large amounts of valuable products generated contribute to value creation in the process, which promotes recycling and can ultimately reduce incineration and landfilling of grinding swarf. The environmental benefits from this recycling approach have recently been verified with LCA in a separate report (Johansson, 2025).

4. Conclusion

A flexible recycling process for producing iron chloride solutions from steel grinding swarf was successfully developed in this study. Up to 95% Fe was extracted from the waste and converted to FeCl_2 by leaching for 3 h at 60°C and $\text{pH} \leq 2$, with an initial L/S = 3 mL/g. Metal dissolution was inhibited by cutting fluids, but leaching of both briquetted and filtered samples showed that briquetted swarf had sufficiently low lubricant content to allow near-complete Fe extraction. Raising the slurry pH to ≥ 4 by adding additional swarf after leaching resulted in hydrolysis and complete precipitation of Cr, Al, and Mo without significant loss of FeCl_2 . Noble metals such as Cu, Ni, and Co were not hydrolyzed but were found to be cemented onto metallic Fe in the swarf. Cementation was found to be more efficient at elevated Cl^- concentrations, where reaction rates were high due to decreased mass transport resistance and increased deposition kinetics. Partial recirculation of FeCl_2 product to the leaching step was therefore proposed to maintain high Cl^- concentrations throughout the process. Emulsified cutting fluids and hydraulic oils were found to aggregate and adsorb onto solids during leaching and could be removed together with

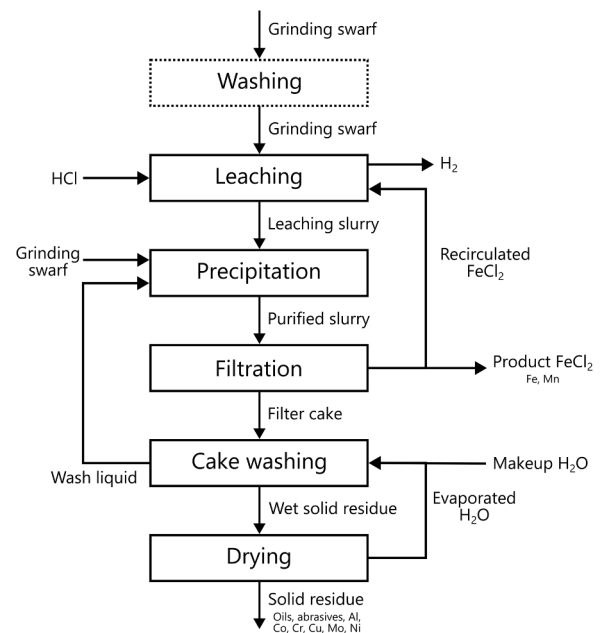


Fig. 5. Proposed recycling process for producing FeCl_2 from grinding swarf.

precipitated metals by filtration of the FeCl_2 product. The final FeCl_2 product met the highest commercial water treatment standards in terms of metal impurity concentrations and was suitable for direct use or as a precursor to FeCl_3 coagulants. This was confirmed by oxidizing FeCl_2 and performing flocculation tests, which showed that the recycled FeCl_3 performed similarly to a commercial magnetite-based FeCl_3 coagulant. Besides coagulants, the recycling process also generates an alloy concentrate and H_2 with potential applications in steel production. These products increase the potential value of grinding swarf, which can ultimately lead to reduced landfilling of this hazardous waste and contribute to increasing circularity within both steel and water treatment industries. Future efforts should be directed at evaluating the economic feasibility of the technology and scaling of individual unit processes to validate their feasibility in an industrially relevant setting. More grinding swarf samples should also be tested to study process limitations in terms of upper alloy and lubricant contents.

CRediT authorship contribution statement

Thomas Ottink: Writing – review & editing, Writing – original draft, Visualization, Validation, Software, Methodology, Investigation, Formal analysis, Data curation, Conceptualization. **Martina Petranikova:** Writing – review & editing, Validation, Supervision, Resources, Project administration, Funding acquisition.

Declaration of competing interest

The authors declare the following financial interests/personal relationships which may be considered as potential competing interests:

Thomas Ottink reports a relationship with Anferra AB that includes: board membership. Thomas Ottink has patent pending to Chalmers Ventures AB. If there are other authors, they declare that they have no known competing financial interests or personal relationships that could have appeared to influence the work reported in this paper.

Acknowledgements

The authors would like to thank Chalmers Material Analysis Laboratory (CMAL) for giving access to their XRD instruments and Andreas Schaefer for his expertise and contribution with XRF analysis. Special

acknowledgement is also extended to Linda Widbro at SKF AB and Anders Krantz at Husqvarna AB for kindly providing swarf samples and insight into the grinding processes and waste management, and Håkan Wiktorsson, Jakob Smusin, Fazlollah Azarnoush, and Bernt Drube at Kemira Kemi AB for inviting us to their facilities and contribution in oxidation and flocculation experiments.

This research was supported by Formas (2021–00449) and ÅForsk (24-368)

Supplementary materials

Supplementary material associated with this article can be found, in the online version, at [doi:10.1016/j.rcradv.2026.200320](https://doi.org/10.1016/j.rcradv.2026.200320).

Data availability

Data will be made available on request.

References

- Addy, S., Fletcher, A.J., 1987. The deposition of cobalt on iron powder by means of the cementation reaction. *Hydrometallurgy* 17, 269–280. [https://doi.org/10.1016/0304-386X\(87\)90058-2](https://doi.org/10.1016/0304-386X(87)90058-2).
- Anacleto, A.L., Carvalho, J.R., 1996. Mercury cementation from chloride solutions using iron, zinc and aluminium. *Miner. Eng.* 9, 385–397. [https://doi.org/10.1016/0892-6875\(96\)00025-8](https://doi.org/10.1016/0892-6875(96)00025-8).
- Atkins, P., de Paula, J., 2002. *Atkins' Physical Chemistry*, 7th Edition. Oxford University Press.
- Azarhoushang, B., 2022. Abrasive tools. *Tribology and Fundamentals of Abrasive machining Processes: third edition* 31–73. <https://doi.org/10.1016/B978-0-12-823777-9.00012-4>.
- Binnemans, K., Jones, P.T., Manjón Fernández, Á., Masaguer Torres, V., 2020. Hydrometallurgical processes for the recovery of metals from steel industry by-products: a critical review. *J. Sustain. Metall.* 6, 505–540. <https://doi.org/10.1007/S40831-020-00306-2>, 2020 6:4.
- Chang, J.I., Lin, J.J., Huang, J.S., Chang, Y.M., 2006. Recycling oil and steel from grinding swarf. *Resour. Conserv. Recycl.* 49, 191–201. <https://doi.org/10.1016/J.RESCONREC.2006.03.014>.
- Crabtree, J.H., Schaefer, W.P., 1966. The oxidation of iron (II) by chlorine. *Inorganic Chemistry* 5 (8), 1348–1351. <https://doi.org/10.1021/ic50042a011>.
- Einar Mattsson, 1996. *Basic Corrosion Technology For Scientists and Engineers*, 2nd Edition. Maney Publishing for IOM3, the Institute of Materials, Minerals and Mining, London, 1996.
- Fu, H., Matthews, M.A., Warner, S.L., 1998. Recycling steel from grinding swarf. *Waste Manage.* 18, 321–329. [https://doi.org/10.1016/S0956-053X\(98\)00042-7](https://doi.org/10.1016/S0956-053X(98)00042-7).
- Grobwendt, F., Bürk, V., Kopanka, B., Jäger, S., Pollak, S., Leich, L., Röttger, A., Petermann, M., Weber, S., 2023. A novel powder-metallurgical eco-friendly recycling process for tool steel grinding sludge. *J. Clean. Prod.* 392, 136329. <https://doi.org/10.1016/J.JCLEPRO.2023.136329>.
- Guimarães, A.P., Maia, D.A.S., Araújo, R.S., Cavalcante Jr, C.L., de Sant'Ana, H.B., 2010. Destabilization and recuperability of oil used in the formulation of concentrated emulsions and cutting fluids. *Chem. Biochem. Eng. Q.* 24, 43–49.
- Hankel, J., Jäger, S., Weber, S., 2020. Development of a recycling strategy for grinding sludge using supersolidus liquid phase sintering. *J. Clean. Prod.* 263, 121501. <https://doi.org/10.1016/j.jclepro.2020.121501>.
- Hess, M.J., Kawatra, S.K., 1999. Environmental beneficiation of machining wastes-part I: material characterization of machining swarf. *J. Air Waste Manage. Assoc.* 49, 207–212. <https://doi.org/10.1080/10473289.1999.10463783>.
- Huang, J.H., Kargl-Simard, C., Oliazadeh, M., Alfantazi, A.M., 2004. pH-controlled precipitation of cobalt and molybdenum from industrial waste effluents of a cobalt electrodeposition process. *Hydrometallurgy* 75, 77–90. <https://doi.org/10.1016/J.HYDROMET.2004.06.008>.
- Hurlen, T., 1975. Kinetics and thermodynamics of Ni/Ni(II) reactions in concentrated solutions of nickel and calcium chlorides. *Electrochim. Acta* 20, 499–505. [https://doi.org/10.1016/0013-4686\(75\)90040-7](https://doi.org/10.1016/0013-4686(75)90040-7).
- Jamett, N.E., Hernández, P.C., Casas, J.M., Taboada, M.E., 2018. Speciation in the Fe (III)-Cl(I)-H₂O system at 298.15 K, 313.15 K, and 333.15 K (25°C, 40°C, and 60°C). *Metall. Mater. Trans. B: Process Metall. Mater. Process. Sci.* 49, 451–459. <https://doi.org/10.1007/S11663-017-1010-0>/FIGURES/4.
- Johansson, K., Liljenroth, A., 2023. Carbon footprints of inorganic coagulants. IVL report U, 6780.
- Johansson, K., 2025. LCA of recovered ferric chloride from grinding swarf: Environmental performance of Anferra's process compared to State-of-the-Art processes.
- Jinxing, J., 1982. *Fundamental Aspects of Nickel Electrowinning from Chloride Electrolytes*. The University of British Columbia, Vancouver.
- Lee, C.M., Choi, Y.H., Ha, J.H., Woo, W.S., 2017. Eco-friendly technology for recycling of cutting fluids and metal chips: a review. *Int. J. Precis. Eng. Manuf. - Green Technol.* 4, 457–468. <https://doi.org/10.1007/S40684-017-0051-9>/METRICS.
- Lee, H., Jung, M., Bae, M., Lee, E., Jin, H., Mishra, B., 2020. Removal of oil from ferrous grinding swarf of automobile industry by aqueous washing process. *Waste Manage.* 111, 51–57. <https://doi.org/10.1016/J.WASMAN.2020.05.020>.
- Incopa, n.d. Iron-based coagulant: a good example of the circular economy. 2020. (accessed: 2026-02-12). <https://www.incopa.org/wp-content/uploads/2020/06/2020-05-29-Incopa-circular-economy-Iron-based-coagulant.pdf>.
- Lienhardt, W.S., 1925. Process of recovering nickel. Assignee: metal & Thermit Corporation, patent application no. 1592307.
- Liu, W., Migdisov, A., Williams-Jones, A., 2012. The stability of aqueous nickel(II) chloride complexes in hydrothermal solutions: Results of UV-Visible spectroscopic experiments. *Geochimica et Cosmochimica Acta* 94, 276–290. <https://doi.org/10.1016/J.GCA.2012.04.055>.
- Makhloufi, L., Saidani, B., Hammache, H., 2000. Removal of lead ions from acidic aqueous solutions by cementation on iron. *Water. Res.* 34, 2517–2524. [https://doi.org/10.1016/S0043-1354\(99\)00405-4](https://doi.org/10.1016/S0043-1354(99)00405-4).
- Miller, J.D., Beckstead, L.W., 1973. Surface deposit effects in the kinetics of copper cementation by iron. *Metall. Trans.* 4, 1967–1973. <https://doi.org/10.1007/BF02665425>/METRICS.
- Morgan, B., Lahav, O., 2007. The effect of pH on the kinetics of spontaneous Fe(II) oxidation by O₂ in aqueous solution – basic principles and a simple heuristic description. *Chemosphere* 68, 2080–2084. <https://doi.org/10.1016/J.CHEMOSPHERE.2007.02.015>.
- Nakamura, K., Hayashi, S., 2006. Grinding sludge recycling to reduce environmental load analysis of disturbing factor for briquetting of Grinding sludge. *Tetsu-to-Hagane* 92, 535–538. <https://doi.org/10.2355/TETSUTOHAGANE1955.92.8.535>.
- Nayström, P., 1998. *Brikettering Av Stål-Och Gjutjärns-spån Samt Slipmull. Gjuteriföreningen*.
- Niu, Z., Li, G., He, D., Fu, X., Sun, W., Yue, T., 2021. Resource-recycling and energy-saving innovation for iron removal in hydrometallurgy: crystal transformation of ferric hydroxide precipitates by hydrothermal treatment. *J. Hazard. Mater.* 416, 125972. <https://doi.org/10.1016/J.JHAZMAT.2021.125972>.
- Ottink, T., Vieceli, N., Foreman, M.R.S.J., Petranikova, M., 2022. Novel approach to recycling of steel swarf using hydrometallurgy. *Resour. Conserv. Recycl.* 185, 106450. <https://doi.org/10.1016/J.RESCONREC.2022.106450>.
- Pearson, R.G., 1963. Hard and soft acids and bases. *J. Am. Chem. Soc.* 85, 3533–3539. <https://doi.org/10.1021/JA00905A001>.
- Rai, D., Sassi, B.M., Moore, D.A., 1987. Chromium(III) hydrolysis constants and solubility of Chromium(III) hydroxide. *Inorg. Chem.* 26, 345–349.
- Ramasahayam, S.K., Guzman, L., Gunawan, G., Viswanathan, T., 2014. A comprehensive review of phosphorus removal technologies and processes. *J. Macromol. Sci. Part A* 51, 538–545. <https://doi.org/10.1080/10601325.2014.906271>.
- Ríos, G., Pazos, C., Coca, J., 1998. Destabilization of cutting oil emulsions using inorganic salts as coagulants. *Colloids. Surf. A Physicochem. Eng. Asp.* 138, 383–389. [https://doi.org/10.1016/S0927-7757\(97\)00083-6](https://doi.org/10.1016/S0927-7757(97)00083-6).
- Sareyed-Dim, N.A., 1974. *The Cementation of Nickel Onto Iron At Elevated Temperatures*. Monash University, Clayton.
- Saylam, H., 1982. *Deposition of Cobalt On Iron Powder*. Sheffield City Polytechnic, Sheffield.
- Sedzimir, J.A., 2002. Precipitation of metals by metals (cementation)—Kinetics, equilibria. *Hydrometallurgy* 64, 161–167. [https://doi.org/10.1016/S0304-386X\(02\)00033-6](https://doi.org/10.1016/S0304-386X(02)00033-6).
- Shen, Y.F., Xue, W.Y., Niu, W.Y., 2008. Recovery of Co(II) and Ni(II) from hydrochloric acid solution of alloy scrap. *Trans. Nonferrous Metals Soc. China* 18, 1262–1268. [https://doi.org/10.1016/S1003-6326\(08\)60214-9](https://doi.org/10.1016/S1003-6326(08)60214-9).
- Swaminathan, K., Subramanian, C., Rao, C.S., 1981. The pressure oxidation of acidic FeCl₂ solution with oxygen. *Hydrometallurgy* 6 (3–4), 339–346. [https://doi.org/10.1016/0304-386X\(81\)90050-5](https://doi.org/10.1016/0304-386X(81)90050-5).
- Webster, J., Tricard, M., 2004. Innovations in abrasive products for precision grinding. *CIRP Annals* 53, 597–617. [https://doi.org/10.1016/S0007-8506\(07\)60031-6](https://doi.org/10.1016/S0007-8506(07)60031-6).
- Wildermuth, E., Stark, H., Friedrich, G., Ebenhöch, F.L., Kühborth, B., Silver, J., Rituper, R., 2000. Iron compounds. *Ullmann's Encyclopedia of Industrial Chemistry*. <https://doi.org/10.1002/14356007.a14.591>.
- Winand, R., 1991. Chloride hydrometallurgy. *Hydrometallurgy* 27, 285–316. [https://doi.org/10.1016/0304-386X\(91\)90055-Q](https://doi.org/10.1016/0304-386X(91)90055-Q).
- Wu, X., Li, C., Zhou, Z., Nie, X., Chen, Y., Zhang, Y., Cao, H., Liu, B., Zhang, N., Said, Z., Debnath, S., Jamil, M., Ali, H.M., Sharma, S., 2021a. Circulating purification of cutting fluid: an overview. *Int. J. Adv. Manuf. Technol.* 117, 2565–2600. <https://doi.org/10.1007/S00170-021-07854-1>, 2021 117:9.
- Wu, X., Li, C., Zhou, Z., Nie, X., Chen, Y., Zhang, Y., Cao, H., Liu, B., Zhang, N., Said, Z., Debnath, S., Jamil, M., Ali, H.M., Sharma, S., 2021b. Circulating purification of cutting fluid: an overview. *Int. J. Adv. Manuf. Technol.* 117, 2565–2600. <https://doi.org/10.1007/S00170-021-07854-1>/TABLES/13.
- World Steel Association, 2022. *World Steel in figures*. (<https://worldsteel.org/data/world-steel-in-figures/world-steel-in-figures-2022/>), accessed: 2026-02-12).
- Xiao, F., Zhang, B., Lee, C., 2008. Effects of low temperature on aluminum(III) hydrolysis: theoretical and experimental studies. *J. Environ. Sci.* 20, 907–914. [https://doi.org/10.1016/S1001-0742\(08\)62185-3](https://doi.org/10.1016/S1001-0742(08)62185-3).